Laser remote sensing of epipelagic fishes

James H. Churnside

NOAA Environmental Technology Laboratory
325 Broadway
Boulder, CO 80303

John R. Hunter

NOAA Southwest Fisheries Science Center
P.O. Box 271
La Jolla, CA 92038

ABSTRACT

Airborne lidar is being considered as a tool for fish detection and for fisheries surveys. Detection has been demonstrated, and an imaging lidar has been developed to detect and identify fish for commercial fisheries. For survey work, a simpler radiometric lidar is being investigated, and preliminary results suggest that such a lidar can be very useful for biomass estimation.

Keywords: lidar, fisheries, ocean optics

1. INTRODUCTION

Airborne remote sensing of fish is not new. Sea birds are very capable of locating fish near the surface of the ocean. Using a similar technique, spotter pilots are used by fishing fleets to locate fish and direct the boats to the fish.[1,2] During the day, fish schools can be directly observed near the surface. At night, the bioluminescence stimulated by the movement of fish is observed. From visual observations, these pilots are able to identify species and to make estimates of school size. These observations are also used by fisheries managers in some cases. For California waters, pilot reports have been collected each year for 30 years to provide a time series of the relative abundance of anchovy, mackerel, and sardine.[1] In the last few years, these data have been used as an index of fish abundance in annual stock assessments.[3]

These airborne data have been valuable to fishery managers because of difficulties with more traditional survey techniques. Traditional direct surveys include ichthyoplankton sampling, trawling, and acoustic surveying. These are limited in coverage area by the speed and cost of surface ships. In addition, many schooling fishes may avoid surface vessels,[4] biasing survey results.

Despite their usefulness, visual observations have several difficulties. The first is that they are severely depth limited. The detection depth limit is about one diffuse attenuation length, although this depends strongly on illumination, sea state, and the skill of the individual observer. Photographic records have been used in an attempt to eliminate observer-to-observer differences.[5,6] These are still subject to illumination and sea state problems.

For these reasons, laser systems are being developed for application in fisheries. Laser illumination will allow penetration to greater depths than passive observations, and range gating will mitigate difficulties caused by the rough air-sea interface.

An airborne fish-lidar also has important commercial fishing applications. In many parts of the world, tuna fisheries (yellowfin and skipjack tuna), and small pelagic fisheries (sardine, anchovy, mackerel, menhaden) employ airplanes or helicopters to locate fish schools for the industry. Substitution of visual observations by a lidar would greatly increase the effectiveness of aerial observations, thereby increasing industry efficiency. In addition, improved aerial fish finding may solve a critical fishery bicatch problem in the yellowfin tuna fishery of the Eastern Tropical Pacific (ETP). In the ETP, tuna are captured by locating dolphin herds, and this methods often produces adverse results, including dolphin mortality. An airborne sensor that could detect and track schools of larger tunas unassociated with dolphins would offer an ecologically sound alternative to the current method.

A rather generic block diagram of a fish lidar is presented in Fig. 1. The laser generates a pulse of light in the blue-green region of the visible spectrum, where the absorption of sea water is minimized. The laser beam is appropriately shaped with optics, represented by a small lens in the figure, and directed through a scanning system. Laser light reflected by fish and by small particles in the ocean is directed into a telescope by the same scanning system, and detected by an optical detector located either at the focal plane or the image plane of the telescope. The resulting electronic signal is sent to a computer after suitable electronic conditioning and digitization.

Three types of lidar systems are possible for application in fisheries, each providing a different view of fish schools. The simplest, *radiometric lidar*, has no scanning system, and the detector is a single element detector. Each pulse provides a full depth profile of the lidar return at a fixed direction from the aircraft, usually just off nadir. As the aircraft moves along, the system provides a two-dimensional picture of fish schools, where one axis is depth and the other is the target strength integrated over the width of swath cut by the lidar. The second type, *imaging lidar*, produces a horizonal image at a fixed depth without scanning. A gated imaging detector is used, and each pulse provides a horizontal image at a depth determined by the setting of the range gate; these images of individual pulses are patched together as the airplane moves to produce a composite image. The third type, *volumetric lidar,* uses a scanning

Fig. 1. Block diagram of a fish lidar system.

system and a single-element detector. Each pulse provides a single profile with depth, but the scanning system is used to construct a volume, or three-dimensional image, from the individual pulses.
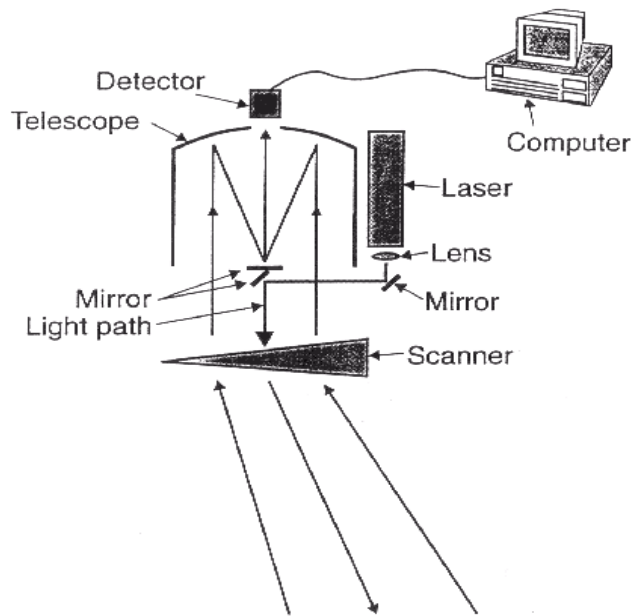
Volumetric lidars have been used for bathymetric applications, as described in other chapters of this volume, and fish have been observed during bathymetric operations. Imaging lidars have been evaluated

for fish finding, and a commercial unit (Fisheye®) is being marketed by Kaman Aerospace. A number of radiometric systems have also been used for fish detection.

2. LIDAR OBSERVATIONS

In 1981, Squire and Krumboltz[7] were among the first to document lidar detection of fish schools. Their system was a Navy radiometric lidar (ORIC) mounted on a helicopter and flown off New Jersey. Reported lidar parameters are provided in Table 1. Fig. 2 is a plot of the vertical cross section of a school inferred from the lidar data. Each numbered section corresponds to a lidar pulse.
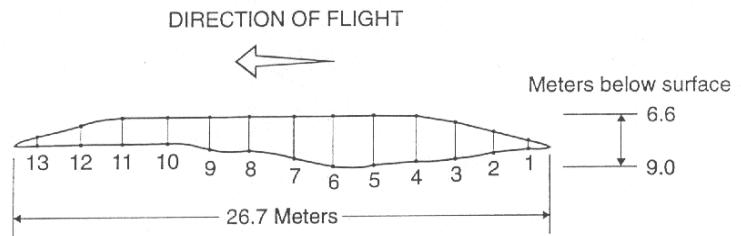

Fig. 2. Vertical cross section of an unidentified fish school from the ORIC lidar (Ref. 7).

Table 1. Parameters of several existing fish lidar systems.

System Name	ORIC	Makrel-2	Osprey®	FLOE	FishEye®
Type	radiometric	radiometric	radiometric	radiometric	imaging
Wavelength	532 nm	532 nm	532 nm	532 nm	532 m
Pulse Length		15 nsec	15 nsec	15 nsec	10 nsec
Pulse Energy		70 mJ	35 mJ	100 mJ	170 mJ
Pulse Repetition Rate	15 Hz	20 Hz	1-20 Hz	10-30 Hz	30 Hz
Laser Divergence	48 mrad	1 mrad	2 mrad	50 mrad	160 mrad
Receiver Aperture Diameter		15 cm	20 cm	20 cm	
Receiver Field of View	48 mrad	2-13 mrad		25 mrad	160 mrad
Electronic Bandwidth		40 MHZ	100 MHZ	100 MHZ	
Shutter Speed					20-120 nsec
Amplifier	linear	linear	logarithmic	logarithmic	linear
Sample Rate		40 MHZ	250 MHZ	1 GHz	30 Hz

Since 1982, the Institute of Atmospheric Optics in Russia has used airborne radiometric lidar to detect fish in the sea. The parameters of their most recent configuration, referred to as the Makrel-2,[8,9] are also presented in Table 1. This system transmits linear polarization and receives both the co-polarized and the cross-polarized return, providing additional information about scattering targets. Fig. 3 is a sample return from the Makrel-2 showing a clear water return (a) and a return including a fish school at a depth of about 11 m (b). The clear water return shows an intensity (curve 1) that decreases with depth and a depolarization ratio (curve 2) that increases with depth. The fish school can be identified by an increase in the received intensity and a decrease in the depolarization ratio at 11 m.

Development of the Osprey® lidar[10] by Remote Sensing Industries began in 1990. This device is a radiometric lidar designed to detect tuna from a helicopter. The parameters of this lidar are also presented in Table 1. The most extensive test of this system occured between September 25 to October 20, 1992, when it was installed on the helicopter of the CMS purse seiner *Captain Vincent Gann*, and operated on a daily basis for a total of approximately 160 hours in the eastern tropical Pacific. Fig. 4 is an example of data obtained during this test. The single-profile display on the left clearly shows a fish return at a depth of 50 feet. This was confirmed to be a school of tuna; the commercial purse seiner harvested this particular school. It contained 2.5 tons of 3-5 kg skipjack and yellowfin tuna, 0.5 tons of bigeye tuna over 2 kg, 31.5 tons of skipjack and yellowfin tuna under 3 kg, 3.2 tons of bigeye tuna under 2 kg, and 0.3 tons of small black skipjack tuna, or a total of 38 tons of tuna. This was one of the larger schools caught on what was not a very successful
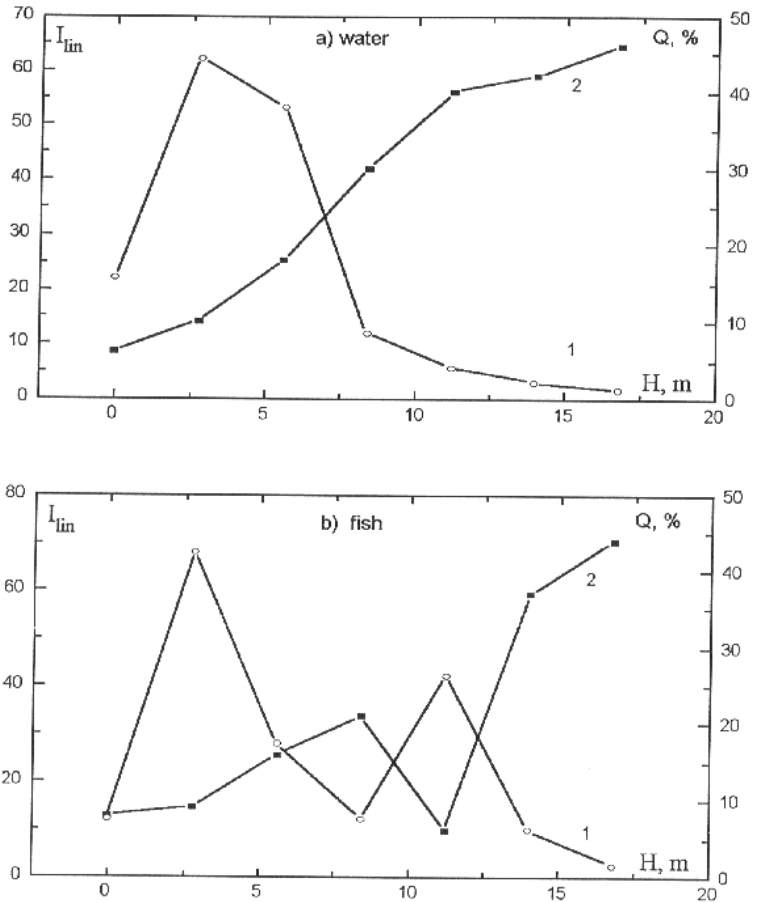

Fig. 3. Depth record of a lidar pulse containing fish at 11 m from the Makrel-2 lidar (Ref. 9). Intensity I_{lin} of the return (curve 1) is on the left vertical axis, and depolarization ratio Q (curve 2) is on the right.
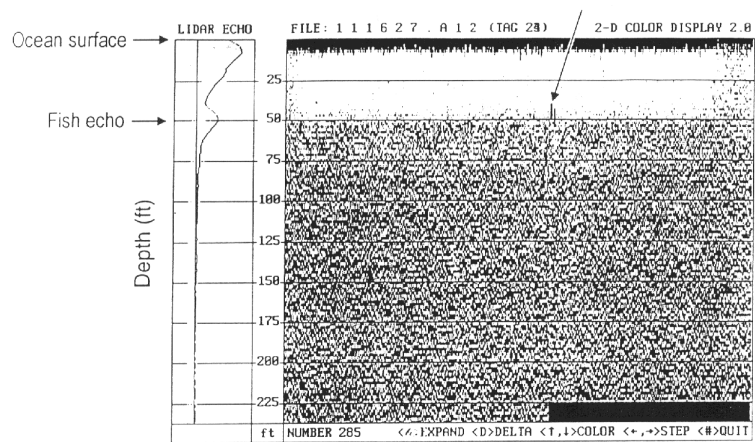

Fig. 4. Depth profile and time/range image containing a tuna school at pulse 285 from the Osprey® lidar (Ref. 10).

cruise.

The National Oceanic and Atmospheric Administration (NOAA) Experimental Oceanic Fish Lidar (FLOE), also a radiometric lidar, is being developed for aerial surveys of epipelagic fishes. Although it is capable of flying in a small aircraft, it has been operated on the research trawler R/T *David Starr Jordan*, which is also equipped with sonar and acoustic echo-sounders. The pertinent parameters are presented in Table 1. Normally, this lidar transmits parallel polarization and receives perpendicular polarization. This seems to provide the best contrast between fish and volumetric scattering in the water column. Fig. 5 is a typical fish-school image from the September 1995 cruise. The top portion of the image is the raw, logarithmic amplifier output. The bottom portion of the image has been processed to separate the fish return from the water return. This processing is not necessary for fish detection, since the enhancement of the signal corresponding to fish is clear in the unprocessed image. However, for quantitative analysis of the magnitude of the fish return, that return needs to be isolated.
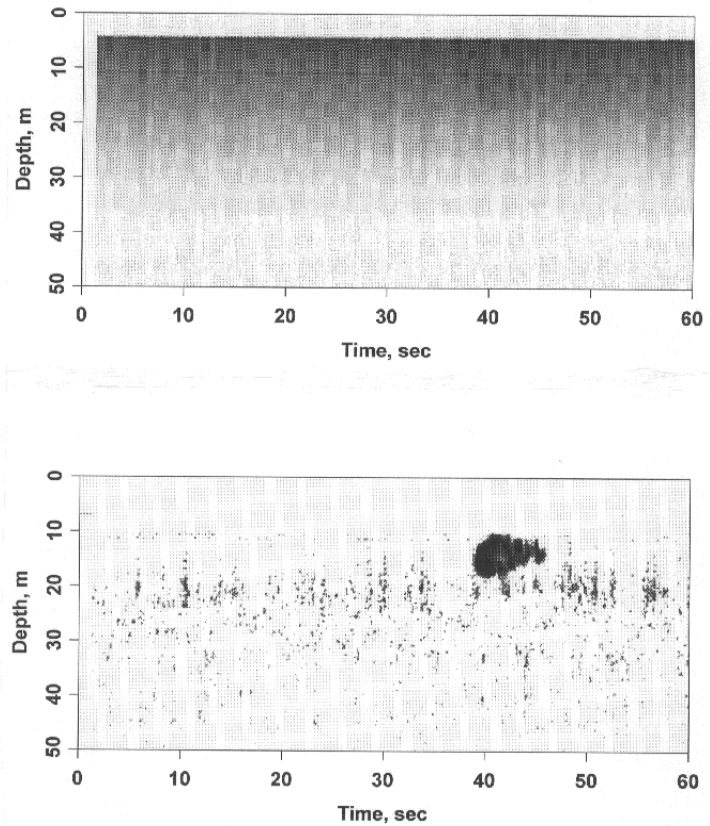

Fig. 5. Time/range image of a fish school from the FLOE lidar. Upper image is the unprocessed image, and the lower image has been processed to separate the fish reflection from the background water reflection.

In the simplest case, we assume that the water properties are constant with depth, so that the return from water only can be expressed as

$$S(z) = a \exp(-\alpha z) / (h + nz)^2 + b, \qquad (1)$$

where S is the linear lidar signal, z is depth, a is a signal amplitude that depends on parameters such as laser energy and pulse width, water backscatter coefficient, receiver aperture, detector responsivity, etc., α is the attenuation coefficient of the laser in the water, h is the height of the lidar above the surface, n is the index of refraction of the water, and b is the contribution of background light to the signal. If fish are present at some depth, there is an additional contribution to the signal at that depth that depends on the backscatter coefficient of the fish, so

$$S(z) = a\left(1 + \frac{\beta_f}{\beta_w}\right) \exp(-\alpha z) / (h + nz)^2 + b, \tag{2}$$

where β_f and β_w are the backscatter coefficients of the fish and of the water. This model also assumes that the attenuation of light by the fish can be neglected.

The processing steps used to obtain the separated image in Fig. 5 follow from these two equations. First, a, α, and b are estimated by choosing three depths on each return that are free of fish and solving the resulting three equations. These three parameters are used with Eq. (1) to obtain an estimate of the water return, S_w. The logarithm of this is subtracted from the logarithm of the measured signal to get

$$\ln(S) - \ln(S_w) = \ln\left(1 + \frac{\beta_f}{\beta_w}\right). \tag{3}$$

Exponentiating this quantity and subtracting 1 provides the fish backscatter coefficient normalized by the water backscatter coefficient. This quantity is proportional to the number of fish within the depth-resolution element.

Fig. 6 is the echo sounder record of the same fish school. Since the two instruments are separated by about 20 m on the ship, the two images of the fish school would not be expected to be identical. It is clear, however, that the general features of school depth, thickness, and fish density are very similar in the two images.
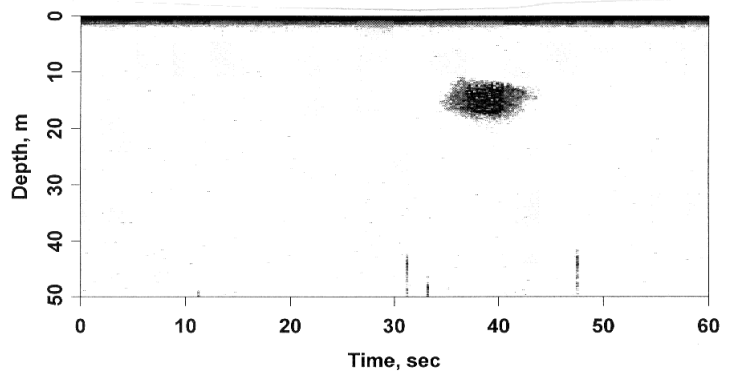

Fig. 6. Echo sounder time/range image of the same school as in Fig. 5.

A scanning lidar, the LARSEN 500, was used to collect data during the 1995 herring fishery off of the east coast of Vancouver Island in Canada.[11] This lidar is not included in Table 1. A sophisticated signal-processing technique was developed to locate fish schools precisely, despite low signal levels.

The FishEye® lidar is an imaging system designed primarily for fish detection. It images the outline of large fish or mammals or the outline of schools. The resolution depends on water clarity, but a few tens of cm is typical. This resolution provides information that can help in species identification, but gives little information on depth. This is disadvantageous for biomass estimation of schooling fish since school thickness is needed for the computation of the biomass of a school. The system is designed so that the gate must be set for a particular depth, and all one can tell is whether the target is above or below that depth.

Targets above the gated depth will appear as a shadow against the water return, those below will appear brighter than the surroundings. This system was extensively tested off the coast of Chile during a three-week period in July 1995. Fig. 7 is a reflection-mode image of a school of fish in the net around a fishing boat. The shadow of the boat is clearly visible on the right of the image. The range gate for this image, and hence the fish school, is from 12 to 26 m. Fig. 8 is a shadow-mode image of another school. The depth gate is the same, so these fish are in the upper 12 m of the ocean.

MISSION:	071295R
SCENE:	20:59:03
LATITUDE:	19'32'49"S
LONGITUDE:	70'13'01"W
ALTITUDE:	1000 FEET
SPEED:	100 KNOTS
GATE DEPTH:	40-85 FEET
SWATH WIDTH:	157 FEET
DISPLAY HEIGHT:	350 FEET

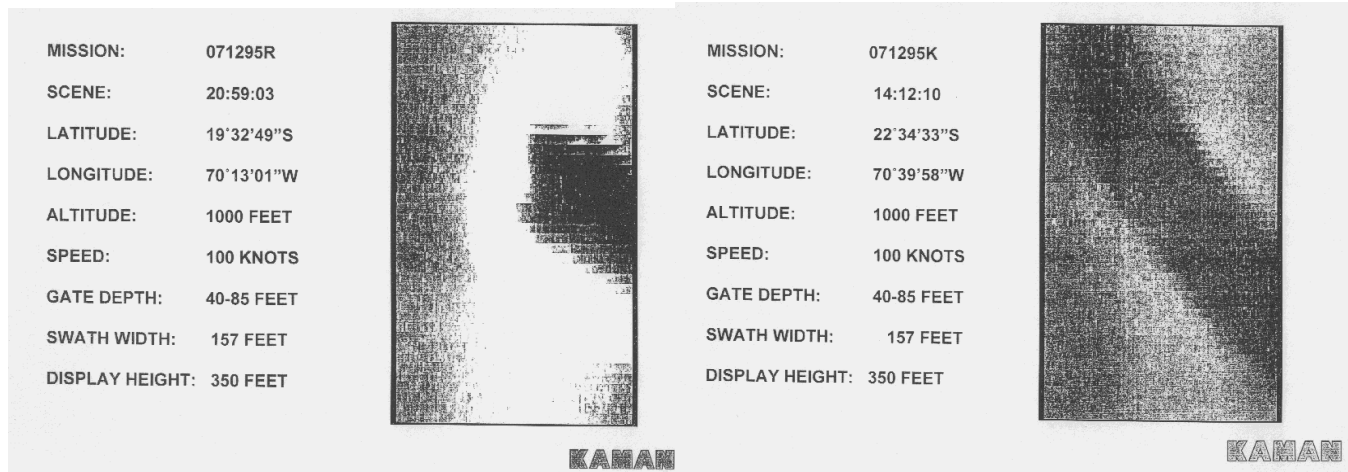| MISSION: | 071295K |
SCENE:	14:12:10
LATITUDE:	22'34'33"S
LONGITUDE:	70'39'58"W
ALTITUDE:	1000 FEET
SPEED:	100 KNOTS
GATE DEPTH:	40-85 FEET
SWATH WIDTH:	157 FEET
DISPLAY HEIGHT:	350 FEET

Fig. 7. Reflection image of a school of anchovies in a net around a fishing boat off Chile from the FishEye® lidar (provided by Kaman Aerospace).

Fig. 8. Shadow image of a school of anchovies off Chile from the FishEye® lidar (provided by Kaman Aerospace).

3. MODELING EFFORTS

Many of the modeling issues relevant to fisheries lidar are the same as those for other lidar systems. However, in this case, the optical characteristics of the fish also need to be determined. In 1974, Murphree, et al[12] concluded, "The results from the developed mathematical model, using input parameters of presently available equipment and estimates of fish school density and reflectivity, reveal that the power received at an airborne detector from fish reflected incident laser radiation and the S/N are of sufficient magnitude to locate fish schools with an airborne remote laser sensing system." The estimates of fish school density and reflectivity used in this study were that 50% of the cross-sectional area of the beam intercepted fish, and that the reflectivity of those fish was 5%. Depths of up to 14 m were considered.

A more recent study[13] used a Monte-Carlo calculation, and also concluded that fish detection was possible. This study considered a layer of fish 5 m thick at a depth of 5 m. This study used a fish reflectivity of 5%, based on Reference 12. Two fish densities were used in this study, 50 m^{-3} and 25 m^{-3}, with an assumed fish cross section of 20 cm^2. For a 5-m thick layer, the product of the number density, the cross-sectional area of each fish, and the layer thickness results in roughly 50% and 25% coverage of the layer by the beam, so that fish density is also similar to that used in Reference 12. Fig. 9 is a plot of depth profiles of the intensity of a lidar return using that model and reproduced from Reference 9.

For many purposes, a much simpler model can be used. A commercial spreadsheet program is ideal

for varying the parameters of a lidar system, the water, or the fish, and observing the consequences. This requires that the physics of the model be simplified. The full effects of multiple scattering are particularly difficult to incorporate into a spreadsheet model that will perform the calculations in a reasonable time. However, in many cases, such effects can be parameterized by, for example, an increased beam divergence. If the initial beam divergence is larger that the beam spreading, even this is not needed. Fig. 10 is a plot of the signal return from a school of fish at a depth of 5 m calculated using such a spreadsheet. In this case, a measured profile of the diffuse attenuation coefficient in the Southern California Bight was used to calculate the return from a system with a fairly wide field of view.
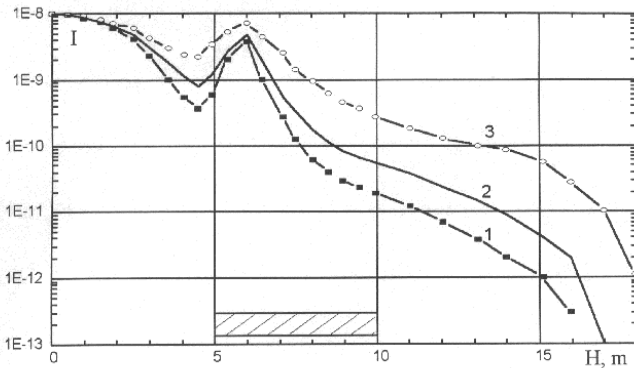

Fig. 9. Monte-Carlo calculations of the depth profiles of lidar returns from a layer of fish at a depth of 5 m (Ref. 9). Fields of view of 2 mrad (curve 1), 4 mrad (curve 2), and 8 mrad (curve 3) were used.
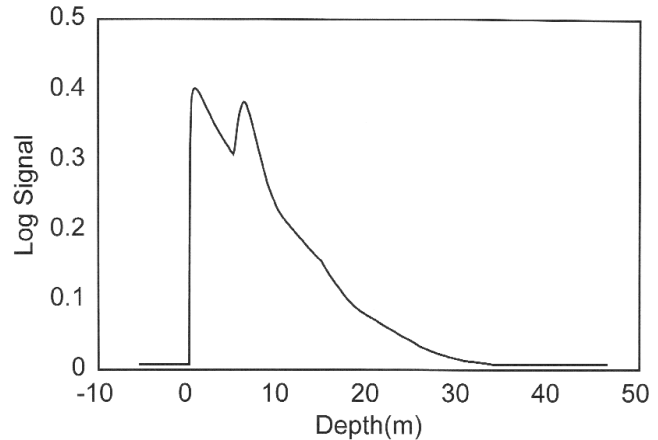

Fig. 10. Commercial spreadsheet calculation of the depth profile of a lidar return from a layer of fish at a depth of 5 m.

3. FISH SCHOOL CHARACTERISTICS

Performance of fish lidar, particularly for fishery management, depends upon the three biological parameters discussed below: fish reflectivity, school packing density, and depth. Fish reflectivity is of key importance not only because it is needed for forecasting maximum fish-detection depth, but, most importantly, because it forms a direct computational link between the strength of the lidar signal and the number of fish or biomass. Squire and Krumboltz[7] assumed a reflectivity of 50% in order to estimate the area of the fish intercepted by their lidar. Krekova, et.al.[13] followed Murphree, et.al.[12] in assuming a reflectivity of 5%. Fredriksson et.al.[14] measured the lidar return from fish, but their system was not calibrated. Benigno and Kemmerer[15] measured the reflectivity of menhaden in the sea using natural light and got a value of less than 1% across the blue-green portion of the spectrum. Churnside and McGillivary[16] made calibrated measurements on dead fish, and obtained reflectivities of 18-26% for blue light and 15-22% for green light, depending on species. Clearly, more work on fish reflectivity is needed.

A direct measure or index of packing density of fish within a school is also essential if school biomass is to be accurately estimated. Packing density of schools is highly variable because it is a function of feeding, fright, swimming behavior, diel rhythms, and other factors. Procedures used to measure packing

density in the sea, such as dropping cameras through schools, counting the fish in purse-seine catches, and driving ships equipped with echo sounders over schools, generally frighten the fish and increase density. The most striking difference is between night and day schools. Night schools are often so diffuse that some researchers have concluded that schooling ceases, although purse-seine fisheries for sardine, anchovy, and menhaden use bioluminescence to detect and catch schools at night.

Clearly, fish size affects packing density, and attempts have been made to express an average packing density in terms of fish length, L.[17,18] Based on laboratory observations, densities of L^{-3} and $(2.44L)^{-3}$ have been suggested (by Refs. 17 and 18, respectively). However, average packing densities in the open ocean are typically much lower than in laboratories. A summary of open-ocean data for sprat, herring, and saithe suggests that the packing density for these fish is lower than either of the laboratory-based models.[19] That is, the nearest neighbor distance is generally less that 2.44L.

Measurements made from underwater photographs demonstrate a large range of packing density under natural conditions. For Northern anchovy during the day, a range of nearest-neighbor distances from 0.79L to 1.63L was measured.[20] This corresponds to packing densities of 50 to 366 fish per cubic meter. For Japanese anchovy at night, nearest-neighbor distances varied from 7.8L to 12L, corresponding to a packing-density range of 0.25 to 0.87 m^{-3}.[21] Jack mackerel, measured at night, had nearest-neighbor distances of 18L to 21.5L and packing densities of 6.6 to 19.5 m^{-3}.[22] Packing density will even vary greatly within a school. One school of herring was found to have densities from fewer than 0.1 m^{-3} to more than 8 m^{-3}.[19] Observations of sardine schools suggest that the leading edge of a crescent-shaped sardine school has a much higher density than the trailing edge.[23]

School packing density also seems to vary greatly between day and night. The average density of the South African pilchard was found to be 4.3 times as great in the day as at night.[30] The typical density of adult anchovy schools was estimated to be 20 times that at night.[24] School thickness does not appear to vary greatly between day and night.[25]

The next parameter to consider is school depth. For most species, some fish will be found at depths that exceed even the most optimistic forecasts for airborne lidar performance, especially during the day. One possible exception may be the Pacific soury, a commercial species that is limited in range to the upper few meters of the water column.

One common feature of the vertical distribution of epipelagic schooling fishes is that the schools are closer to the surface at night. This has been documented by acoustic records off daily migration of fish from greater depths to the surface at night[26] and by surface observations.[27] The swimming patterns of yellowfin tuna tracked with acoustic transmitters[28] show depth changes of 100 m several times in an hour. These data also show that the daytime vertical range was between 50 and 150 m, while the nighttime range was between 0 and 100 m in depth.

The diurnal difference in depths seems to be related to the amount of light required for the fish to see each other. Whitney[29] reviewed data on visual thresholds for schooling and concluded that sufficient light existed in the sea for schooling to continue at night if the fish were close enough to the surface. This implies that the nighttime depth of schooling is a function of ambient light, water clarity, and species. Fig. 11 is a plot of the visual threshold for schooling as a function of chlorophyll concentration for northern

anchovy.[30]   Note that as the chlorophyll concentration increases, the maximum depth penetration of a lidar is expected to decrease. Under these conditions, the fish will come closer to the surface where they can more easily be detected.

Even during the day, sardines appear to stay relatively close to the surface. Three echo-sounder surveys of sardine depth distributions off Japan[31] found 99.1%, 93.2%, and 92.9% of the fish in the upper 26 m of the ocean. Anchovy range somewhat deeper. Three daytime acoustic surveys of anchovies off California[4] found 75%, 65%, and 70% of the fish within the upper 50 m. Depth distributions of the larvae of four species in the Southern California Bight have been approximated by the Weibull distribution:

$$k(z) = K\left[1 - \exp\left(\frac{z}{z_0}\right)^{\tau}\right], \qquad (4)$$

where k is the biomass per unit area in the upper z meters, K is the total biomass per unit area, z_0 is the mean depth, and τ is a shape parameter (unity for the exponential distribution). The parameters for the four species are listed in Table 2.

One of the most variable aspects of fish schools is size. No evidence exists that schools concentrate around a certain optimum size. In some boreal coastal pelagic fishes, such as herring, saithe,
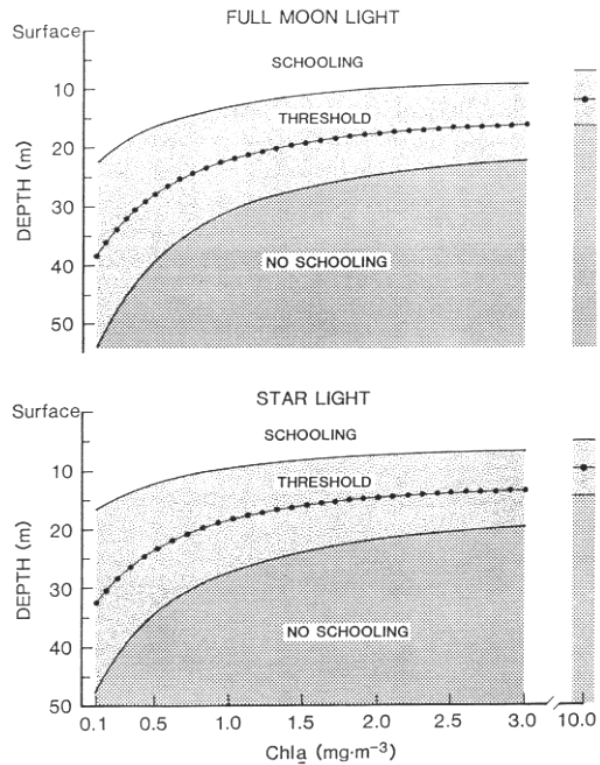

Fig. 11. Estimates of the maximum depth of northern anchovy schools at night from Ref. 27 for two illumination conditions and varying chlorophyll concentrations. Darkly shaded area indicates where no schooling is expected; lightly shaded area indicates depth range of schooling threshold, with the geometric mean indicated by the dotted line.

Table 2. Fitted parameters of the Weibull distribution for depth distribution of four species of fish in the Southern California Bight.

Species	K (kg/10m²)	z_0	τ
Anchovy	0.414	33.56	1.2
Hake	0.033	90	5
Pacific Mackerel	0.00026	5	1
Sardine	0.13	10	1

and sprat, school sizes vary by a factor of 10,000 or more.[19] Similarly, the areas of daytime anchovy schools range from less than 5 m² to more than 50,000 m². Small schools are by far the most numerous, but most of the biomass of a stock may be concentrated in relatively rare, very large schools. For example, cumulative frequency distributions of the horizontal areas of schools indicate that 50% of anchovy schools are less than 30 m in diameter, and 90% of the total area of all schools was produced by schools larger than 30 m.[32] Another study[24] reported that most anchovy schools were 5-30 m in diameter and 4-15 m thick. While these smaller schools were common all year, larger schools, with 25-30 m diameters and 12-40 m thick, appeared in fall and winter.

While the size of a school is often described in terms of a diameter, schools are not always circular. They can be described as ovoid, ameboid, ribbon like, and crescent shaped. The advancing edge of crescent-shaped schools is often convex.[23] Nighttime anchovy schools tend to be more elongated that daytime schools.[27] Accelerated swimming can cause ovoid schools to become more elongated.[33] Epipelagic fish schools also tend to be larger in horizontal extent than in thickness. Echo sounder measurements of sardine schools provided a mean school thickness that varied between 3.4 m and 3.9 m for different surveys, with nearly all schools less than 10 m thick.[34,35] The median thickness of anchovy schools appears to be about 4 m, but values range up to 19 m.[4] One estimate of school shape from older data suggests that a length:width:thickness relationship of 3:2:1 is not uncommon.[17] More recent measurements of the mean ratio of the "crosswise" horizontal dimension to thickness for nine surveys of herring, saithe, and sprat obtained values of 1.7 to 4.7, with a median ratio of 2.6.[19] This report pointed out that schools tend to become thinner when they get close to either the surface or the bottom, and tend to be more spherical in open water; schools within a few meters of the surface had length-to-thickness ratios as large as ten. Anchovy schools also are very thin at night, when they are close to the surface.[27]

An additional factor to consider is that schools of pelagic fishes are often arranged in distinct aggregations called shoal groups or school groups.[5,36,37] These groups have definite coherence, such that the presence of one group will decrease the probability of another group within 13-17 km. These groups will move considerable distances as a unit. This patchiness affects the design of an aerial survey or search.

3. SURVEY DESIGN CONSIDERATIONS

An optimal survey minimizes potential biases, while delivering the greatest statistical precision within cost constraints. A fundamental assumption of resource surveys is that the surveyed area encloses all or nearly all of the stock under consideration. This assumption is violated frequently because survey boundaries are set by costs rather than habitat boundaries. Visual or passive-imaging aerial surveys can minimize the survey area bias in the horizontal dimensions because of their low cost per survey mile, but they produce a large bias in the vertical dimension because of the limited depth penetration. Airborne lidar surveys can also minimize the horizontal area bias, and greatly reduce the vertical or volume bias for daylight surveys. At night, it is possible that most pelagic species (mackerel, anchovy, sardines, menhaden, and possibly tuna) may be fully recruited into a lidar survey volume.

For some time to come, accurate fish identification in aerial surveys may remain restricted to about 1 attenuation length and the identity of lidar targets detected below that depth will depend on local knowledge and voucher specimens. Similarly, acoustic surveys usually include trawling for approximate identification of acoustic targets and specimens for determining age composition and growth. In

ichthyoplankton surveys (fish eggs and larvae), on the other hand, species are identified absolutely. If an estimate of absolute biomass is the needed, the ideal approach may be to combine lidar surveys with acoustic and/or ichthyoplankton surveys. Acoustic and airborne lidar surveys are quite complementary. Echo sounders mounted on ship hulls cannot be used for targets in the upper 5-10 meters of the ocean, and side-looking sonars are also not effective in same region because of surface and wave inference. The depth range of target overlap between lidar and acoustic methods, about 10-40 meters, allows intercalibration between acoustics and lidar. Another interesting contrast is that acoustics are most effective during the day when schools are deeper, while night may be the preferred time for lidar because schools may be fully recruited into the surveyed volume. Nighttime lidar surveys are also less effected by background light. Both methods need trawling to confirm species identification .

There is also merit in combining airborne lidar surveys with ichthyoplankton surveys. Because fewer assumptions are required, ichthyoplankton methods, particularly daily egg production (DEP) and related methods,[37] are potentially the most accurate for estimating biomass of epipelagic fishes but they are also the most costly. Vessel progress is slow because of frequent stops to take plankton tows (a tow every 4 nautical miles is recommended), and the vessel must also be used for trawling, since specimens are needed to estimate the weight-specific production of eggs. Airborne lidar and DEP methods might profit greatly from being combined. The slow DEP method could be greatly enhanced by a rapid method for discovering spatial boundaries, while the absolute abundance estimates provided by the DEPM may be best way to covert school targets into biomass. In addition, the sampling effort on board the vessel could be allocated on the basis of the abundance of lidar detected fish schools. Such an adaptive sampling strategy would greatly improve the precision of the biomass estimate. Similar arguments were advanced by Shelton et.al.[38] who developed methods for combining DEP surveys with acoustics and trawls. These authors stressed the value of combining absolute abundance estimates of relatively low precision, provided by their DEP estimate, with the relatively precise measurement of relative abundance provided by acoustics. This combined method has been in routine use in South Africa for over a decade.

The optimal lidar survey design should also include satellite data, since the scale and continuous nature of the aerial transects make them ideally suited to defining habitat boundaries using remotely sensed quantities such as temperature and ocean color. These quantities can easily be measured from the aircraft in addition to the satellite data. The would reduce the variance introduced by the steady state assumptions necessary for a long ship survey. The major benefits of including ocean sensing in the aerial survey design include improved sampling strategies that reduce survey cost and risk and increased precision of the estimate through the use of geostatistics and the adaptive sampling strategies mentioned above.

The optimal approach to developing a lidar survey technology is for the instruments and the survey design to evolve together. This requires modeling. Lo and Hunter (in prep) have simulated the performance of a hypothetical airborne lidar in detecting several species in the Southern California Bight. One question was whether a scanning system would be required to obtain a sufficient swath width on each transect. The move from a radiometric lidar to a scanning lidar involves significant costs. First, the scanning system itself presents some significant costs. It also adds weight to the system and requires power. More importantly, the laser pulse repetition rate has to be significantly increased to provide a full cross-track scan in the time a radiometric lidar provides only a single pulse. Not only is the laser more expensive because of its higher average power, but it also is heavier and requires more power for operation and cooling. Finally, a more

expensive data-acquisition system is needed to handle the higher data rates. Not only are the initial system costs higher, the added weight and power requirements mean that a larger aircraft is needed for the surveys, thus increasing the operating costs.

Fig. 12 is a plot of the simulation results of lidar detection probability for anchovies in the Southern California Bight. The total habitat area for these simulations is 13,500 square nautical miles, and the total number of fish schools within this habitat varies from 16,000 to 320,000. The swath width was varied from 10 cm, about the width of an unmodified laser beam, to 900 m, about the width of the field of view of a visual observer.[39] In this simulation, the lidar was assumed to detect any schools within the swath width. The results show the probability of detecting a school during a single transect perpendicular to the coastline. The increase in detection probability with increasing swath width is small; the detection probability is largely determined by the size of fish school groups rather than the size of the lidar swath. This suggests that a radiometric lidar is probably the most cost effective for this application.

A lidar will not detect any school within its swath width; however, the detection probability will decrease with depth because of the attenuation of light. Because of the exponential nature of the attenuation, the return signal decreases rapidly with depth. Assuming a high signal level near the surface, the signal level makes the transition from well above the noise level to lost in the noise very quickly. It thus makes sense to consider the detection probability as unity above the penetration depth and effectively zero below this depth. The penetration depth, of course, will depend on the characteristics of the lidar, of water column, the fish, and the signal processing.

Fig. 13 is a plot of detection probability as a function of penetration depth of the lidar for the depth distributions of Pacific mackerel, sardine, anchovy, and hake as approximated in Eq. (4). For a penetration depth of 20-30 m, mackerel and sardine
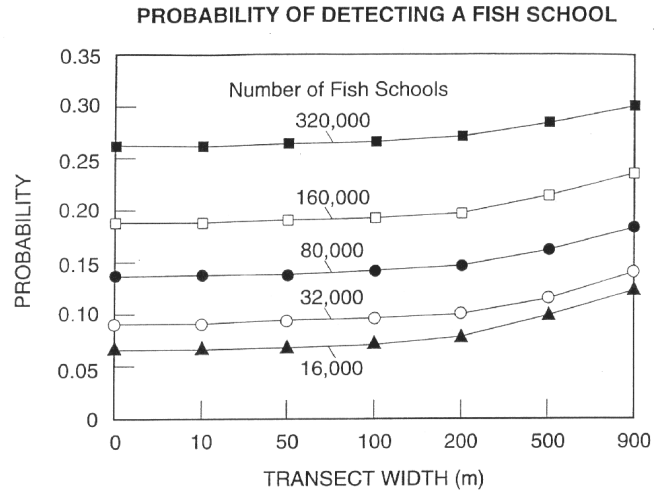

Fig. 12. Simulation results of the probability of detecting an anchovy school with an ideal lidar during a transect as a function of the transect swath width for several values of the total number of anchovy schools in the Southern California Bight.
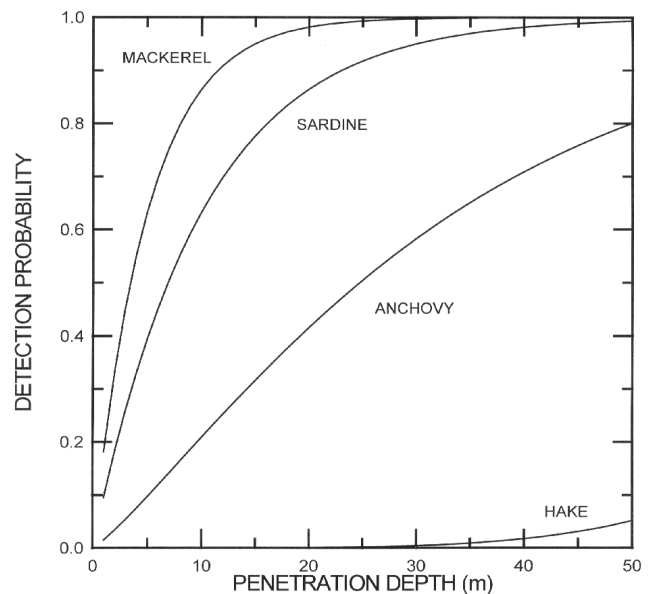

Fig. 13. Plot of lidar detection probability as a function of lidar penetration depth for four species common to the Southern California Bight.

can be fairly reliably detected, and about half of the anchovy will be detected. Lidar is probably not a useful tool for hake surveys. The probability of detecting a school during a transect is the product of the detection probability as calculated for this figure and the detection probability from a calculation like that which produced Fig. 12. In other words, the total detection probability P(det) is the product of the probability that a school is within the beam P(school) and the probability that a school is detected given that it is within the beam P(det|school). For a survey of anchovy with a stock of 100,000-200,000 schools, the probability of detecting a school on a single transect of the Southern California Bight would therefore be about 8-10%.

6. SUMMARY

The detection of fish schools by lidar has been demonstrated in the field and the magnitude of the signal has been estimated by models. Based on this information, modeling of the performance of lidar as a fisheries management tool has begun. Although it is early in the investigation, it appears that lidar can be an important tool in the management of several species of epipelagic fishes. An optimal survey might include ship transects with acoustics and direct sampling, supplemented by aircraft transects over a much larger portion of the habitat. Determination of the extent of the habitat could be aided by sea-surface temperature and ocean-color images provided by satellite. A small aircraft (perhaps six-passenger) could be outfitted with a radiometric lidar and also with a small infrared radiometer and color video. These last instruments would allow the interactions between fish, sea-surface temperature, and ocean color to be studied in more detail, so that determination of habitat from satellite images could be made more accurate. Ideally, the pilot would be an expert fish spotter who could provide reliable information about fish species for visually observable schools.

7. ACKNOWLEDGEMENTS

8. REFERENCES

1. N.C.H. Lo, L.D. Jacobson, and J.L. Squire, Jr., "Indices of Relative Abundance from Fish Spotter Data Based on Delta-Lognormal Models," Can J. Fish. Aquat. Sci. **49**, 2515-2526, 1992.
2. J.L. Squire, Jr., "Apparent Abundance of Some Pelagic Marine Fishes off the Southern and Central California Coast as Surveyed by an Airborne Monitoring Program," Fish. Bull. U.S. **70**, 1005-1019, 1972.
3. J.T. Barnes, L.D. Jacobson, A.D. MacCall, and P. Wolf, "Recent Population Trends and Abundance Estimates for the Pacific Sardine (*Sardinops Sagax*)," Calif. Coop. Oceanic Fish. Invest. Rep. **33**, 60-75, 1992.
4. D.V. Holliday and H.L. Larsen, "Thickness and Depth Distributions of Some pelagic Fish Schools off Southern California," Fish. Bull. **77**, 489-494, 1979.
5. D.L. Cram and I. Hampton, "A Proposed Aerial/Acoustic Strategy for Pelagic Fish Stock Assessment," J. Const. Int. Explor. Mer. **37**, 91-97, 1976.

6. B.S. Nakashima and G.A. Borstad, "Detecting and Measuring Pelagic Fish Schools using Remote Sensing Techniques," ICES Report C.M. 1993/B:7 Session T, Fish Capture Committee, 1993. 18pp.

7. J.L. Squire, Jr. and H. Krumboltz, "Profiling Pelagic Fish Schools using Airborne Optical Lasers and Other Remote Sensing Techniques," Mar. Tech. Soc. J. **15**, 443-448, 1981.

8. A.I. Abramochkin, V.V. Zanin, I.E. Penner, A.A. , Tokhomirov, and V.S. Shamanaev, "Airborne Polarization Lidars for Atmospheric and Hydrospheric Studies," Atmos. Opt. **1**, 92-96, 1988.

9. G.P. Kokhanenko, M.M. Krekova, I.E. Penner, V.S. Shamanaev, and J.H. Churnside, "Search of Schools of Fish by Polarization Lidar from a Board of a Plane," Second International Airborne Remote Sensing Conference, San Francisco, California, 24-27 June, 1996.

10. CW. Oliver, W.A. Armstrong, and JA Young, "Development of an Airborne Lidar System to Detect Tunas in the Eastern Tropical Pacific Purse-Seine Fishery," NOAA Technical Memorandum NOAA-TM-NMFS-SWFSC-204, NOAA Southwest Fisheries Science Center, P.O. Box 271, La Jolla, California, 92038, June, 1994. pp 67.

11. S.R. Pillai and A. Antoniou, "Vertical Thickness and Depth Distribution of Fish Schools Using Lidar Technology," Second Internation Airborne Remote Sensing Conference, San Francisco, California, 24-27 June, 1996.

12. D.L. Murphree, C.D. Taylor, and R.W. McClendon, "Mathematical Modeling for the Detection of Fish by an Airborne Laser," AIAA J. **12**, 1686-1692, 1974.

13. M.M. Krekova, G.M. Krekov, I.V. Samokhvalov, and V.S. Shamanaev, "Numerical Evaluation of the Possibilities of Remote Laser Sensing of Fish Schools," Appl. Opt. **33**, 5715-5720, 1994.

14. K. Fredriksson, B. Galle, K. Kyström, S. Svanberg, and B. Öström, "Underwater Laser-Radar Experiments for Bathymatry and Fish-School Detection," Göteborg Institute of Physics Report GIPR-162, 1978. 28 pp.

15. J.A. Benigno and D.J. Kemmerer, "Aerial Photographic Sensing of Pelagic Fish Schools: A Comparison of Two Films," Proc. ASC Symp. on Remote Sens. in Ocean., Lake Buena Vista, Florida, 1973.

16. J.H. Churnside and P.A. McGillivary, "Optical Properties of Several Pacific Fishes," Appl. Opt. **30**, 2925-2927, 1991.

17. T.J. Pitcher and B.L. Partridge, "Fish School Density and Volume," Mar. Biol. **54**, 383-394 (1979).

18. L.I. Serebrov, "Relationship Between School Density and Size of Fish," J. Ichthyol. **16**, 135-140 (1976).

19. O.A. Misund, "Dynamics of Moving Masses: Variability in Packing Density, Shape and Size among Herring, Sprat, and Saithe Schools," ICES J. Mar. Sci. **50**, 145-160 (1993).

20. J. Graves, "Photographic Method for Measuring Spacing and Density within Pelagic Fish Schools at Sea," Fish. Bull. U.S. **75**, 230-234 (1977).

21. I. Aoki and T. Inagaki, "Photographic Observations on the Behaviour of Japanese Anchovy *Engraulis Japonica* at Night in the Sea," Mar. Ecol. Prog. Ser. **43,** 213-221 (1988).

22. I. Aoki, T. Inagaki, and L.V. Long, "Measurements of the Three-Dimensional Structure of Free-Swimming Pelagic Fish Schools in a Natural Environment," Bull. Jap. Soc. Sci. Fish. **52**, 2069-2077 (1986).

23. I. Hara, "Moving Direction of Japanese Sardine School on the Basis of Echo Sounder Surveys," Bull. Tokai Reg. Fish. Res. Lab. **51**, 1939-1945 (1985).

24. I. Hampton, J.J. Agenbag, and D.L. Cram, "Feasibility of Assessing the Size of the South West

Africal Pilchard Stock by Combined Aerial and Acoustic Measurements," Fish. Bull. S. Afr. **11**, 10-22 (1979).

25. P.E. Smith, "I. Pelagic Fisheries: General Features. II. Larval Anchovy Patchiness. III. Sampling to Determine Anchovy Larval Mortality in the Sea," in *Marine Fish Larvae: Morphology, Ecology, and Relation to Fisheries,* R. Lasker, ed. (University of Washington Press, Seattle, 1981) pp. 2-31.

26. K.F. Mais, "Pelagic Fish Surveys in the California Current," Calif. Dept. Fish game, Fish. Bull. **162**, 1-79 (1974).

27. J.L. Squire, Jr., "Northern Anchovy School Shapes as Related to Problems in School Size Estimation," Fish. Bull., U.S. **76**, 443-448 (1978).

28. T. Yonimori, "Stude of Tuna Behavior, Particularly their Swimming Depths, by the use of Sonic Tags," Newsl. Enyo (Far Seas) Fish. Res. Lab. Shimizu **44**, 1-5 (1982).

29. R.R. Whitney, "Schooling of Fishes Relative to Available Light," Trans. Amer. Fish. Soc. **98**, 497-504 (1969).

30. J.R. Hunter and R. Nicholl, "Visual Threshold for Schooling in Northern Anchovy *Engraulis Mordax*," Fish. Bull., U.S., **83**, 235-242 (1985).

31. I. Hara, "Shape and Size of Japanese Sardine School in the Waters off the Southern Hokkaido on the Basis of Acoustic and Aerial Surveys," Bull. Jap. Soc. Sci. Fish. **51**, 41-46 (1985).

32. R.P. Hewitt, P.E. Smith, and J.C. Brown, "Development and Use of Sonar Mapping for Pelagic Stock Assessment in the California Current Area," Fish. Bull., U.S. **74**, 281-300 (1976).

33. J.H.S. Vlaxter and J.R. Hunter, "The Biology of Clupeoid Fishes," Adv. Mar. Biol. **20**, 1-223 (1982).

34. I. Hara, "Estimation of Fish Density Using the Line Intercept Method," Bull. Jap. Soc. Sci. Fish. **49**, 1619-1625 (1983).

35. I. Hara, "Distribution and School Size of Japanese Sardine in the Waters off the Southeastern Coast of Hokaido on the Basis of Echo Sounder Surveys," Bull. Tokai Reg. Fish. Res. Lab. **113**, 67-78 (1984).

36. P.E. Smith, "Precision of Sonar Mapping for Pelagic Fish Assessment in the California Current," J. Const. Int. Explor. Mer. **38**, 33-40 (1978).

37. J.R. Hunter and N.C.-H Lo, "Ichthyoplankton Methods for Estimating Fish Biomass: Introduction and Terminology," Bull. Mar. Sci. **53**, 723-727, 1993.

38. P.A. Shelton, M.J. Armstrong, and B.A. Roel, "An Overview of the Application of the Daily Egg Production Method in the Assessment and Management of Anchovy in the Southeast Atlantic," Bull. Mar. Sci. **53**, 778-794, 1993.

39. P.C. Fiedler, "The Precision of Simulated Transect Surveys of Northern Anchovy, *Engraulis Mordax*, School Groups," Fish. Bull., U.S. **76**, 679-685 (1978).